Neutralizing human monoclonal antibodies binding multiple serotypes of botulinum neurotoxin

C.Garcia-Rodriguez[1], I.N.Geren[1], J.Lou[1], F.Conrad[1], C.Forsyth[1], W.Wen[1], S.Chakraborti[1], H.Zao[1], G.Manzanarez[1], T.J.Smith[2], J.Brown[2], W.H.Tepp[3], N.Liu[4], S.Wijesuriya[4], M.T.Tomic[4], E.A.Johnson[3], L.A.Smith[2] and J.D.Marks[1,5]

[1]Department of Anesthesia and Pharmaceutical Chemistry, University of California–San Francisco, Rm 3C-38, San Francisco General Hospital, 1001 Potrero Ave., San Francisco, CA 94110, USA, [2]Integrated Toxicology Division, United States Army Medical Research Institute of Infectious Diseases, Fort Detrick, MD 21702, USA, [3]Department of Food Microbiology and Toxicology, University of Wisconsin, Madison, WI 53706, USA and [4]XOMA (US) LLC, 2710 Seventh St., Berkeley, CA 94710, USA

[5]To whom correspondence should be addressed.
E-mail: marksj@anesthesia.ucsf.edu

Botulism, a disease of humans characterized by prolonged paralysis, is caused by botulinum neurotoxins (BoNTs), the most poisonous substances known. There are seven serotypes of BoNT (A–G) which differ from each other by 34–64% at the amino acid level. Each serotype is uniquely recognized by polyclonal antibodies, which originally were used to classify serotypes. To determine if there existed monoclonal antibodies (mAbs) capable of binding two or more serotypes, we evaluated the ability of 35 yeast-displayed single-chain variable fragment antibodies generated from vaccinated humans or mice for their ability to bind multiple BoNT serotypes. Two such clonally related human mAbs (1B18 and 4E17) were identified that bound BoNT serotype A (BoNT/A) and B or BoNT/A, B, E and F, respectively, with high affinity. Using molecular evolution techniques, it proved possible to both increase affinity and maintain cross-serotype reactivity for the 4E17 mAb. Both 1B18 and 4E17 bound to a relatively conserved epitope at the tip of the BoNT translocation domain. Immunoglobulin G constructed from affinity matured variants of 1B18 and 4E17 were evaluated for their ability to neutralize BoNT/B and E, respectively, *in vivo*. Both antibodies potently neutralized BoNT *in vivo* demonstrating that this epitope is functionally important in the intoxication pathway. Such cross-serotype binding and neutralizing mAbs should simplify the development of antibody-based BoNT diagnostics and therapeutics.

Keywords: botulism/botulinum neurotoxin/molecular evolution/single-chain Fv/yeast display

Introduction

Botulism is caused by botulinum neurotoxin (BoNT; Centers for Disease Control, 1998) the most poisonous substance known (Gill, 1982). The crystal structure of BoNTs (Lacy et al., 1998; Eswaramoorthy et al., 2001; Kumaran et al., 2009) show three functional domains comprising a heavy chain (H_C) and a light chain (L_C; Simpson, 1980; Montecucco and Schiavo, 1995; Lacy et al., 1998). The C-terminal portion of the heavy chain (H_C) is the binding domain that docks the toxin to sialoganglioside receptors and a protein receptor on presynaptic neurons, resulting in toxin endocytosis (Dolly et al., 1984; Dong et al., 2006; Mahrhold et al., 2006). The translocation domain (H_N), at the N-terminal portion of the heavy chain, mediates escape of the toxin L_C from the endosome. Depending on serotype, the L_C cleaves one or more members of the SNARE complex of proteins, blocking acetylcholine release (Schiavo et al., 1992, 1993).

There are seven serotypes of BoNT, serotypes A–G. Naturally occurring human botulism is caused by BoNT serotypes A (BoNT/A), B, E and F and is characterized by flaccid paralysis which, if not fatal, requires prolonged hospitalization in an intensive care unit and mechanical ventilation. Besides causing naturally occurring botulism, BoNTs are also classified by the Centers for Disease Control and Prevention as one of the six highest-risk threat agents for bioterrorism (Arnon et al., 2001). Both Iraq and the former Soviet Union produced BoNT for use as weapons (United Nations Security Council, 1995; Bozheyeva et al., 1999), and the Japanese cult Aum Shinrikyo attempted to use BoNT for bioterrorism (Arnon et al., 2001). It appears that any of the seven BoNT serotypes could cause intoxication via intentional aerosol release (Middlebrook, 1997).

As a result of these threats, there is an urgent need for rapid and very sensitive diagnostic assays that can detect BoNTs, as well as therapies that are safe, effective and can be produced in large quantities for stockpiling (NIAID Experts Panel, 2004). There are a number of assays under development, and many of these rely on high-affinity polyclonal or monoclonal antibodies (mAbs; Varnum et al., 2006; Bagramyan et al., 2008; Kalb et al., 2008, 2009; Grate et al., 2009; Warner et al., 2009). Treatment of botulism also relies on the administration of antibodies. Historically, such antitoxins have been polyclonal antitoxins prepared from either immunized humans or horses (Arnon et al., 2001). More recently, antitoxins comprised of mAbs have been pursued for the treatment of botulism (Amersdorfer et al., 1997, 2002; Nowakowski et al., 2002).

Thus, mAbs are an important resource for the detection, diagnosis and treatment of botulism. Their development is complicated by the fact that there are seven serologically distinct BoNT serotypes which differ by 34–64% at the amino acid level (Lacy and Stevens, 1999; Smith et al., 2007). Polyclonal sera raised against one serotype does not cross react with other serotypes. Moreover, no mAbs have been reported which bind to more than one BoNT serotype. Within serotypes, multiple subtypes exist that differ by 1.6–32% at the amino acid level (Smith et al., 2005; Hill et al.,

2007). Such subtype variability impacts antibody binding and neutralization (Smith *et al.*, 2005; Garcia-Rodriguez *et al.*, 2007). Identification of mAbs capable of binding multiple serotypes could simplify the development of BoNT diagnostics and therapeutics by reducing the number of antibodies required.

For this work, we evaluated a panel of 35 mAbs binding BoNT/A, B and E to identify whether any of the mAbs could bind more than one serotype. Two clonally related mAbs were identified which bound either BoNT/A and B or BoNT/A, B, E and F. These mAbs potently neutralized BoNTs *in vivo* and bound nearly identical conserved epitopes at the tip of the BoNT H_N. The results demonstrate that useful mAbs binding multiple BoNT serotypes, while rare, do exist and suggest an important functional role for the tip of the H_N.

Results

Identification and initial characterization of cross-reactive BoNT mAbs

To identify mAbs binding multiple BoNT serotypes, we studied a panel of 35 antibodies binding BoNT/A, B or E (Supplementary Table S1). Thirty three mAbs were generated from humans immunized with an investigational vaccine containing BoNT/A, B, C, D and E (pentavalent botulinum toxoid), and two mAbs were generated from a mouse immunized with BoNT/A holotoxin (S25 and C25). All mAbs were isolated from single-chain variable fragment (scFv) gene libraries generated from immune B-cells and displayed on either the surface of phage or the surface of yeast (Amersdorfer *et al.*, 1997, 2002; Levy *et al.*, 2007, and unpublished data). mAbs binding to BoNT/A, B or E were then isolated by flow sorting libraries on holotoxin. Seven mAbs were isolated which bound BoNT/A, 18 mAbs were isolated which bound BoNT/B and 10 mAbs were isolated which bound BoNT/E. Within each serotype, mAbs binding each of the three functional toxin domains (H_C, H_N and L_C) were isolated (Supplementary Table S1).

Each mAb was displayed on the surface of yeast as an scFv and evaluated for binding to BoNT/A, B and E by flow cytometry using 100 nM BoNT/A, B or E. If an mAb bound more than one BoNT serotype, then the yeast-displayed scFv was evaluated for its ability to bind each of the seven BoNT serotypes. Where binding was observed, the equilibrium binding constant was measured by flow cytometry. Of all the mAbs studied, two mAbs, 1B18 and 4E17, were identified that bound multiple BoNT serotypes; 1B18 bound BoNT/A and B with affinities of 6.19 and 7.3 nM, respectively (Table I). 4E17 bound BoNT/A, B, E and F with affinities of 1.34, 100, 14.1 and >1000 nM, respectively (Table I). Neither mAb bound BoNT/C, D or G. Alignment of the sequences of 1B18 and 4E17 indicated that these mAbs have highly homologous heavy-chain variable region (V_H) gene segments, V_H CDR3 and V_L gene segments (Fig. 1). Both mAbs are derived from the same IGHV3-7*01 V_H gene segment, IGHJ5*02 J_H gene segment and IGKV1-39*01 kappa light-chain variable region (V_k) gene segment (IGMT database, http://imgt.cines.fr/IMGT_vquest/share/textes). While IGMT assigns the D gene segment to different D genes (IGHD6-19*01 and IGHD3-3*01 for 1B18 and 4E17,

Table I. Affinities of cross-serotype binding yeast-displayed scFv for BoNT

Toxin type	Antibody affinity K_D ($\times 10^{-9}$ M^{-1})			
	BoNT/A	BoNT/B	BoNT/E	BoNT/F
1B18	6.19	7.3	NB	NB
2B18.1	62.4	0.64	NB	NB
4E17	1.34	100	14.1	>1000
4E17.1	0.09	28	0.23	16.8
4E17.2	1.4	27	4.8	2.11
4E17.4	0.33	0.95	0.29	18.6

K_D were measured by using flow cytometry. NB, no binding observed at a concentration of 100 nM BoNT

respectively), D gene assignment can be inaccurate; we hypothesize that the high homology of the V_H CDR3 and identity of the other gene segments indicate that these two antibodies are clonally related.

Impact of increasing mAb affinity for one serotype on cross-serotype specificity

To generate more sensitive antibodies for BoNT detection and more potent antibodies for treatment of botulism, we evaluated the ability to increase antibody affinity (see Fig. 2 for overview). To increase the affinity for BoNT/B (1B18), E (4E17) or F (4E17), diversity was introduced into their respective scFv genes by V_L shuffling (Clackson *et al.*, 1991; Figini *et al.*, 1994). The resulting yeast-displayed scFv libraries were sequentially sorted on decreasing concentrations of either BoNT/B (1B18-based library) or BoNT/E or F (4E17-based library) until the diversity had collapsed to a few sequences (Fig. 2). Individual colonies were sequenced and characterized with respect to binding affinity to identify the highest affinity scFv to either BoNT/B (2B18.1) or BoNT/E or F (4E17.1 and 4E17.2; Table I). To determine the impact of increasing affinity for one serotype on cross-serotype reactivity, the equilibrium dissociation constant (K_D) of yeast-displayed 2B18.1, 4E17.1 and 4E17.2 scFv were measured for BoNT/A, B, E and F (Table I).

For 2B18.1, affinity for the toxin used for selection, BoNT/B, increased 11.4-fold ($K_D = 0.64$ nM) compared with the parental 1B18, whereas that for BoNT/A decreased 10-fold to 62.4 nM. For 4E17.1, the affinity for the toxin used for selection, BoNT/E, increased 61-fold ($K_D = 0.23$ nM) compared with the parental 4E17, whereas that for BoNT/A increased 15-fold to 0.09 nM. The affinity of 4E17.1 for BoNT/B increased 4-fold and that for BoNT/F increased 59-fold compared with 4E17. Finally, for 4E17.2, the affinity for the toxin used for selection, BoNT/F, increased >475-fold ($K_D = 2.1$ nM) compared with the parental 4E17, whereas that for BoNT/A, B and E were approximately the same as 4E17.

In the above experiments, higher affinity antibodies to a specific serotype were generated by flow sorting using only that BoNT serotype. In some instances, high-affinity binding was maintained or increased for other serotypes; in other instances, affinity decreased. To more effectively select for serotype cross reactivity, a selection strategy was utilized where the yeast-displayed scFv library was sequentially sorted on different BoNT serotypes. Specifically, we sought to increase the affinity of 4E17 for BoNT/B, the serotype for

Fig. 1 Amino acid sequence alignment of cross-serotype binding antibodies. The V_H and V_k genes of cross-serotype reactive scFv were aligned. CDR, complementarity determining region; FR, framework region. CDR and FR defined according to IGMT (http://imgt.cines.fr/IMGT_vquest/share/textes).
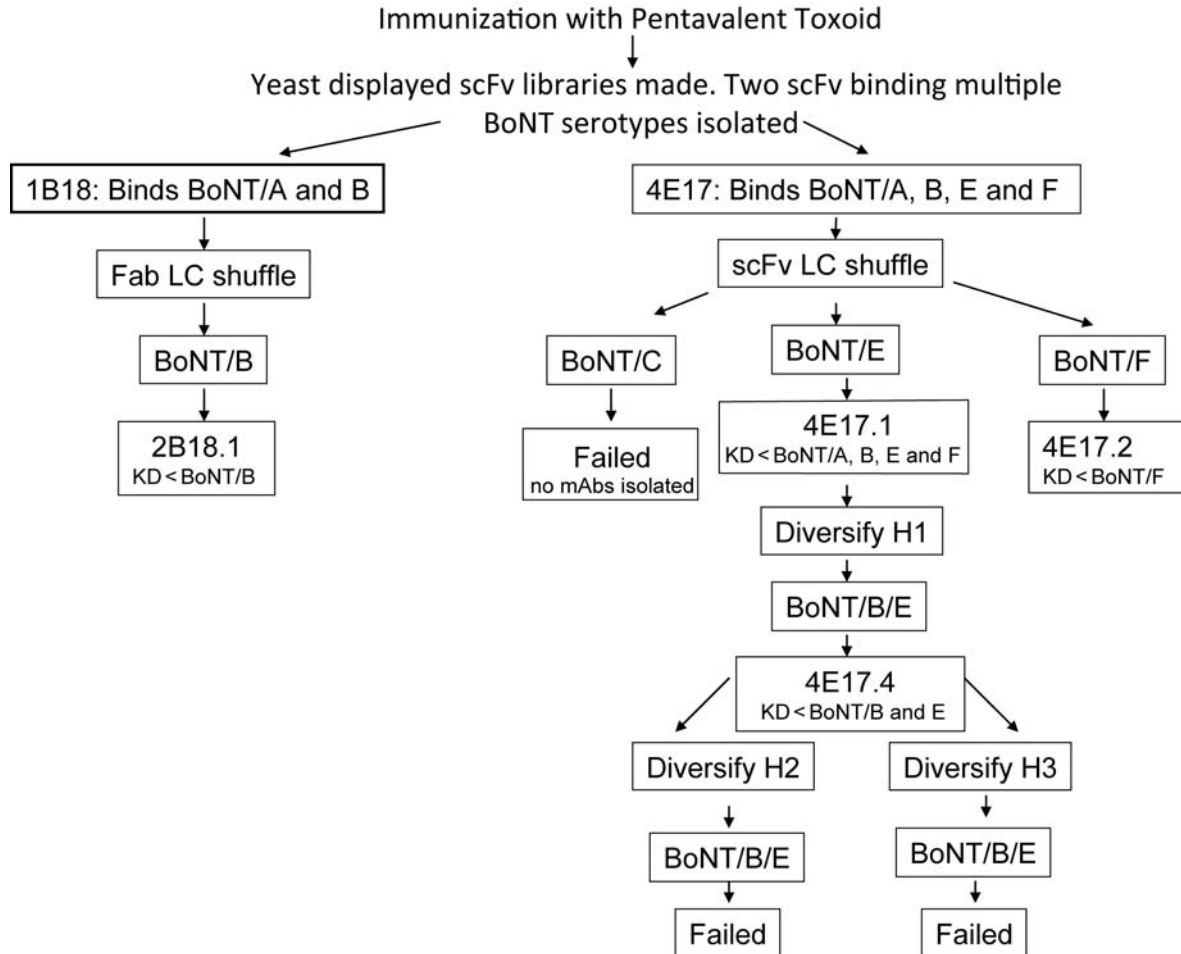
Fig. 2 Strategies used to increase affinity and broaden specificity of 1B18 and 4E17 antibodies. The method used to introduce diversity is indicated (L_C shuffling using the Fab or scFv format or by creating libraries of VHCDR1, VHCDR2 or VHCDR3 mutants). The BoNT serotype used for selection is also indicated. Where more than one serotype is indicated, selections were done sequentially on the serotypes indicated. The selection outcome is also indicated: $K_D <$ BoNT/X indicates that higher affinity antibodies were generated to the BoNT serotypes indicated. No mAbs isolated indicates that no mAbs binding BoNT/C were isolated. Failed indicates that no antibodies were generated that had higher affinities for BoNT/B and E than 4E17.4.

which it has the lowest affinity, while maintaining high-affinity binding to BoNT/E. Diversity was introduced into the 4E17.1 scFv gene by partially randomizing five amino acids in V_H CDR1 (Garcia-Rodriguez et al., 2007; Fig. 2). The resulting yeast-displayed 4E17.1 scFv library was sequentially sorted for four rounds, first on BoNT/B and then on BoNT/E until the diversity had collapsed to a few sequences. Individual colonies were sequenced and characterized with respect to binding affinity to identify the scFv with the highest affinity for BoNT/B and a ratio of K_D for

BoNT/B to E closest to 1.0 (scFv 4E17.4). Affinity of 4E17.4 for BoNT/B increased 32-fold ($K_D = 0.95$ nM) compared with 4E17, whereas that for BoNT/E was essentially unchanged ($K_D = 0.29$ nM; Table I). High-affinity binding was maintained for BoNT/A ($K_D = 0.33$ nM). The results indicate that using this selection strategy, it was possible to broaden high-affinity binding of 4E17 to an additional serotype. To further increase affinity for BoNT/B and E, diversity was introduced into the 4E17.4 scFv gene by partially randomizing five amino acids in V_H CDR2 or V_H CDR3 and

selections performed sequentially on BoNT/B and E as described above (Fig. 2). No clones with higher affinity for both BoNT/B and E were isolated.

Impact of conversion of scFv to immunoglobulin G on affinity for BoNT

For many applications, such as diagnostic ELISA-based assays as well as *in vivo* BoNT neutralization studies, it is either necessary or desirable to utilize immunoglobulin G (IgG; Nowakowski *et al.*, 2002; Varnum *et al.*, 2006; Kalb *et al.*, 2008). We therefore converted the 1B18, 2B18.1, 4E17.1, 4E17.2 and 4E17.4 yeast-displayed scFv to full-length IgG consisting of the human gamma 1 constant region and the human kappa or lambda constant region (Nowakowski *et al.*, 2002). Stable Chinese hamster ovary (CHO) DG44 cell lines were established for each of the antibodies and IgG was purified from cell culture supernatant. The monovalent K_D was determined for each IgG using kinetic exclusion analysis (Kinexa).

Monovalent solution IgG affinities for BoNT were generally equal to or higher than affinities measured for yeast-displayed scFv (Table II). For 1B18 and 2B18.1 IgG, K_D for BoNT/A and B were ∼10-fold higher than the K_D measured for scFv. For 4E17-based IgG, K_D for BoNT/A subtypes were 10–50-fold higher than the K_D measured for scFv, whereas those for BoNT/B, E and F were within a few fold of the K_D measured for scFv. We have previously observed higher affinities for IgG compared with scFv and attributed this to the greater stability of IgG, as well as potential limits in the ability to quantitate affinities significantly <100 pM for yeast-displayed scFv (Razai *et al.*, 2005; Garcia-Rodriguez *et al.*, 2007). For BoNT/A, B and E, affinities were also measured for a number of BoNT subtypes (Hill *et al.*, 2007). For both 1B18- and 4E17-based IgG, affinities were comparable for the three BoNT/A, four BoNT/B and four BoNT/E subtypes studied, with the exception of the non-proteolytic BoNT/B4 (Table II). For BoNT/B4, 1B18 and 4E17.1 had ∼30- and 2000-fold higher affinity, respectively, than for the other BoNT/B subtypes. Taken together, the above results suggest that the 1B18/4E17 epitope is

conserved among the BoNT/A, B and E subtypes, with the exception of BoNT/B4.

Epitope mapping of mAbs 1B18 and 4E17.1

Considering that 1B18 and 4E17 appear to be clonally related antibodies, we hypothesized that they bound identical or nearly identical epitopes that would significantly overlap. To confirm this, we used a sandwich assay where yeast-displayed 1B18 scFv was used to capture BoNT/A or B and the ability of 4E17.1 or a BoNT-specific IgG binding a non-overlapping epitope was measured. 4E17.1 was utilized as 4E17 IgG did not exist. As hypothesized, 1B18 and 4E17.1 cannot bind BoNT/A or B simultaneously (Fig. 3).

To identify the epitope bound by the 1B18 and 4E17 family of mAbs, we stained yeast-displayed BoNT H_C, H_N and L_C domains with 1B18 or 4E17.1 IgG. Both antibodies bound only to the H_N domain, 1B18 binding the BoNT/A and B H_N and 4E17.1 binding the BoNT/A, B and E H_N (Fig. 4). To identify the fine epitope of these mAbs, we aligned the H_N sequences of the seven BoNT serotypes and inspected them for regions that were conserved in BoNT/A, B, E and F, but those which were disparate in BoNT/C, D and G. We identified one such region between amino acids 750 and 758 of BoNT/A, corresponding to amino acids 738 and 746 of BoNT/B and 723 and 731 of BoNT/E (Lacy and Stevens, 1999; Table III). Although the sequence in this region is also generally conserved within subtypes, note that there is a single amino acid difference between BoNT/B4 and the other BoNT/B subtypes at position 743. In BoNT/B4, this amino acid is glutamate, as in BoNT/A, whereas in the other BoNT/B subtypes, this residue is a lysine. This difference could explain why 4E17.1 binds BoNT/B4 with significantly higher affinity than the other BoNT/B subtypes, supporting this site as the epitope for 1B18 and 4E17.

To determine whether this was the region of the 4E17 and 1B18 epitope, the sequence of the BoNT/A H_N between amino acids 750 and 758 (YNQYTEEEK) was replaced with the homologous BoNT/C sequence (YKKYSGSDK). No binding of 4E17.1 IgG was seen to the hybrid BoNT/A H_N containing the BoNT/C sequence (data not shown). To further delineate the epitopes of 1B18 and 4E17.1, single alanine mutations were generated for amino acids 750–758 in BoNT/A, 738–746 of BoNT/B and 723–731 of BoNT/E H_N. This region in the sequence of BoNT/A, B and E is shown in Table III. Each alanine mutant H_N was displayed on the surface of yeast and the affinity of the 1B18 fragment antigen binding (Fab; for BoNT/B H_N mutants) and 4E17.1 Fab (for BoNT/A and E) measured. Comparison of each K_D to wild type allowed the calculation of the change in free energy of binding that occurred upon truncation of the amino acid side chain ($\Delta\Delta G$; Table IV). One mutation at the same position in the loop (E757A for BoNT/A, E744A for BoNT/B and E730A for BoNT/E) had the greatest impact on 1B18 and 4E17.1 binding (Table IV and Fig. 5 for 1B18 and 4E17.1 Fab binding to BoNT/B wild-type H_N and E744A H_N). In the case of 1B18, the mutation E744A completely knocked out binding, whereas mutations S754A, E756A and K758A had a significant impact on binding (Table IV and Fig. 5). For 4E17.1, the mutation E757A also had the greatest impact on binding to both BoNT/A ($\Delta\Delta G = 5.83$) and BoNT/E (no binding observed; Table IV and Fig. 5). Unlike for 1B18 binding to BoNT/B, no other alanine

Table II. Solution equilibrium binding constants for 1B18- and 4E17-based IgG

Toxin type	Antibody affinity K_D ($\times 10^{-12}$ M^{-1})				
	1B18	2B18.1	4E17.1	4E17.2	4E17.4
BoNT/A1 Hall	864	6233	1.83	2.00	39.8
BoNT/A2 Honey	—	—	7.98	—	—
BoNT/A3 Loch Maree	—	—	4.51	—	—
BoNT/B1 okra	545	63	43 760	>100 000	3410
BoNT/B2 213B	818	181	41 330	—	—
BoNT/B3 657	976	91	45 210	—	—
BoNT/B4 Eklund 17B	21	312	16.52	—	—
BoNT/E1 German Sprats	NB	NB	730	1110	291
BoNT/E2 CDC 5247	—	—	205	—	—
BoNT/E3 Alaska	—	—	241	1440	404
BoNT/E4 BL5262	—	—	260	—	—
BoNT/F Langeland	NB	NB	65 080	664	8660

K_D were measured for the different BoNT serotypes and subtypes by flow fluorimetry in a KinExA. NB, no binding; —, not measured.
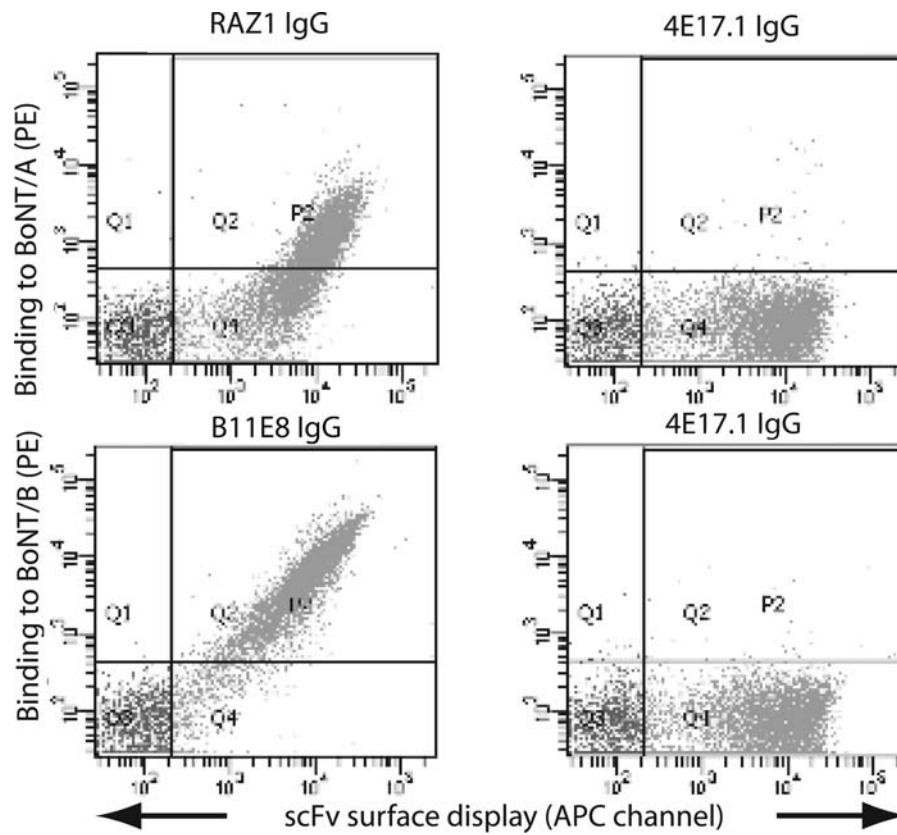
Fig. 3 1B18 and 4E17 bind overlapping epitopes. Yeast-displayed 1B18 scFv was incubated with either BoNT/A (top two panels) or BoNT/B (bottom two panels) followed by incubation with either 4E17.1 IgG or the BoNT/A antibody RAZ1 or the BoNT/B antibody B11E8. 4E17.1 and 1B18 cannot simultaneously bind BoNT/A or B.
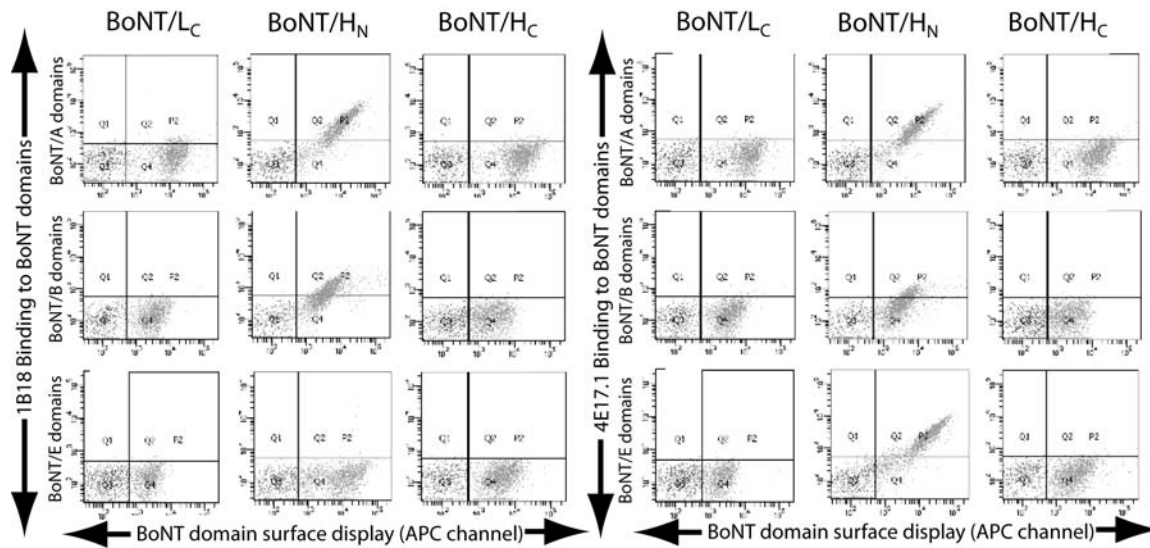
Fig. 4 Mapping the binding site of 1B18 and 4E17.1 mAbs by using yeast-displayed BoNT domains. The H_C, H_N and L_C domains of BoNT/A, B and E were displayed on the surface of yeast and stained with 1B18 or 4E17.1 IgG. The level of BoNT domain display was quantitated using a mAb to a SV5 epitope tag fused to the C-terminus of the domain. Both mAbs bound only to the H_N (1B18 to BoNT/A and B H_N and 4E17.1 to BoNT/A, B and E H_N).

mutation resulted in a $\Delta\Delta G > 1.0$ for 4E17.1 binding to either BoNT/A or E. Alignment of the X-ray crystal structures of BoNT/A, B and E at the epitope indicates that there are both significant similarities and differences in the epitope structures (Fig. 6). All three epitopes are located at the tip of the H_N, consistent with images of 4E17.1 binding to BoNT/

E obtained by single particle electron microscopy (Fischer et al., 2008). There are differences, however, in the number and location of energetically important H_N amino acid side chains. This can be seen most clearly for BoNT/A E757 and the corresponding glutamate residue in BoNT/B and E (Fig. 6, bottom panels).

325

Table III. Sequence of the putative 4E17 epitope in different BoNT serotypes and subtypes

Subtype	Strain	NCBI/GenBank ID	Sequence
BoNT/A1	Hall	ABS38337	**YNQYTEEEK**
BoNT/A2	FRI-honey	AAX53156	– – – – – – – – –
BoNT/A3	Loch Maree	ABA29017	– – – – – – – – –
BoNT/A4	CDC 657	ACQ51417	– – – – – – – – –
BoNT/A5	H0 4402 065	ACG50065	– – – – – – – – –
BoNT/B1	okra	ACA46990	– – I – S – K – –
BoNT/B2	213B	ABM73972	– – I – S – K – –
BoNT/B3	CDC 795	ABM73977	– – I – S – K – –
BoNT/B4 (np)	Eklund 17B	ABM73987	– – I – S – – – –
BoNT/Ba4-B	CDC 657	ABM73986	– – I – S – K – R
BoNT/Bf-B	CDC 3281	CAA73967	– – I – S – K – R
BoNT/B6	Osaka05	BAF91946	– – I – S – K – –
BoNT/E1	German Sprats	BAB86845	– – S – – L – – –
BoNT/E2	CDC 5247	ABM73981	– – S – – L – – –
BoNT/E3	Alaska E43	ABM73980	– – S – – L – – –
BoNT/E4	ATCC 43755	CAA43998	– – S – – L – – –
BoNT/E5	LCL 155	BAB03512	– – S – – L – – –
BoNT/E6	K36	CAM91142	– – S – – L – – –
BoNT/Fprot	Langeland	ABS41202	– – N – – SD – R
BoNT/Fnp	202F	AAA23263	– – N – – SD – –
BoNT/Fbaratii	ATCC 43756	CAA48329	– – N – – LD – –
BoNT/Af-F	strain 84	ACR54282	– – S – – SD – –
BoNT/Bf-F	CDC 3281	CAA73972	– – N – – SD – –
BoNT/C1	Stockholm	BAE47784	– KK – SGSD –
BoNT/C/D	003-9	BAD90568	– KK – SGSD –
BoNT/D	1873	EES90380	– KK – SGSD –
BoNT/D/C	VPI 5995	ABP48747	– KK – SGSD –
BoNT/G	113/30	CAA52275	– – R – S – – D –

Alignment of H_N amino acid sequences in all BoNT serotypes and subtypes for residues 750–758 of BoNT/A, residues 737–745 of BoNT/B and residues 723–731 of BoNT/E (Lacy and Stevens, 1999). The amino acid sequence is relatively conserved in serotypes bound by 4E17.1 (BoNT/A, B, E and F) compared with those serotypes not bound by 4E17.1 (BoNT/C, D and G). Serotypes, strain and NCBI/GenBank accession number are indicated.

Table IV. Affinities and $\Delta\Delta G$ of alanine-substituted BoNT H_N mutants

4E17.1 Fab on BoNT/A H_N			4E17.1 Fab on BoNT/E H_N			1B18 Fab on BoNT/B H_N		
Mutant	K_D (pM)	$\Delta\Delta G$	Mutant	K_D (pM)	$\Delta\Delta G$	Mutant	K_D (pM)	$\Delta\Delta G$
Wild type	16	—	Wild type	88	—	Wild type	780	—
Y750A	27	0.3	Y723A	75	−0.1	Y737A	360	−0.4
N751A	11	−0.2	N724A	84	0.0	N738A	2090	0.6
Q752A	15	−0.4	S725A	81	−0.5	I739A	136 000	3.0
Y753A	NE	—	Y726A	NB	>6	Y740A	NE	—
T754A	NE	—	T727A	180	0.4	S741A	157 000	3.1
E755A	13	−0.1	L728A	100	0.1	E742A	1530	0.4
E756A	67	0.8	E729A	227	0.6	K743A	65	−1.5
E757A	361	5.8	E730A	NB	>6	E744A	NB	>6
K758A	9	−0.3	K731A	111	0.1	K745A	17250	1.8
Wild type	28							
N759A	30	0.1						
N760A	21	−0.1						
I761A	31	0.1						
N762A	26	0.0						
F763A	35	0.1						
N764A	38	0.2						
I765A	22	−0.1						
D766A	15	−0.3						

The dissociation equilibrium constant (K_D) for 1B18 or 4E17.1 F_{ab} was calculated for each yeast-displayed BoNT H_N alanine mutant. The difference in binding free energy ($\Delta\Delta G_{ala-wt}$) between the alanine-substituted and wild-type (wt) H_N was calculated according to the formula $\Delta\Delta G = RTln(K_{D,Ala}/K_{D,wt})$. NE, no H_N surface expression, precluding measurement of K_D and calculation of $\Delta\Delta G$. The K_D of 4E17.1 Fab for BoNT/A H_N mutants was measured in two separate experiments (one experiment for amino acids 750–758 and one experiment for amino acids 759–766), each with their own measurement of wild-type K_D, which differed slightly. NB, no binding.

Potency of in vivo BoNT neutralization by mAbs 2B18.1 and 4E17.1

Given the conservation of 1B18/4E17 binding across serotypes and subtypes, we wondered whether the epitope was associated with biology relevant to intoxication. To evaluate this, we compared the potency of BoNT/B and E neutralization *in vivo* by mAbs 2B18.1 and 4E17.1, respectively, to the non-neutralizing BoNT/B mAb B6.1 (Lou *et al.*, 2010). For both BoNT/B and E, 25 μg of 2B18.1 and 4E17.1 completely protected mice challenged with 200 mouse lethal doses 50% (LD_{50}) of BoNT/B or E, respectively (Fig. 7), indicating that mAb binding to this epitope must interfere with one of the steps leading to intoxication. In contrast, the mAb 4B6.1 showed minimal prolongation in the time to death in mice challenged with BoNT/B.

Discussion

Here, we have shown that it is possible to identify mAbs that bind multiple serotypes of BoNT with high affinity. Of 35 mAbs studied, only two clonally related mAbs bound multiple serotypes; we can find no examples in the literature of such cross-serotype binding BoNT antibodies. That such mAbs are rare is consistent with the less than 63% identity between different BoNT serotypes (Lacy and Stevens, 1999) and the fact that polyclonal sera uniquely define each

'serotype'. In fact, the identity between the different serotypes recognized by the mAbs described here ranges between 36 and 63%. The cross-reactive mAbs bound to a relatively conserved epitope at the tip of the BoNT H_N. This is a functionally important epitope for intoxication, as mAb binding leads to potent BoNT neutralization. We have previously shown that 4E17.1 can block translocation of the BoNT/E L_C *in vitro*, preventing the L_C from reaching its site of action (Fischer *et al.*, 2008). Others have shown that mAbs can bind BoNT, be carried into the pre-synaptic neuron and prevent biologic activity of the toxin. We hypothesize that this is the mechanism by which 2B18.1 and 4E17.1 neutralize toxin *in vivo*; they bind to BoNT are carried into the neuron and block L_C translocation.

Using molecular evolution techniques, it was possible to further broaden the cross reactivity of the 4E17.1 antibody. By sequentially selecting on BoNT/B and E, it proved possible to increase the affinity of 4E17.1 for BoNT/B by 29-fold while maintaining high-affinity binding to BoNT/A and E. However, we were unable to further increase affinity while maintaining cross reactivity. Although the epitope of 1B18 and 4E17 is relatively conserved across the serotypes they bind, there were significant structural differences in the epitopes, especially with respect to the position of the most energetically important amino acid, E757. The crystal structures of BoNT/A, B and E holotoxins are of relatively low resolution and many atoms of the side chains (including
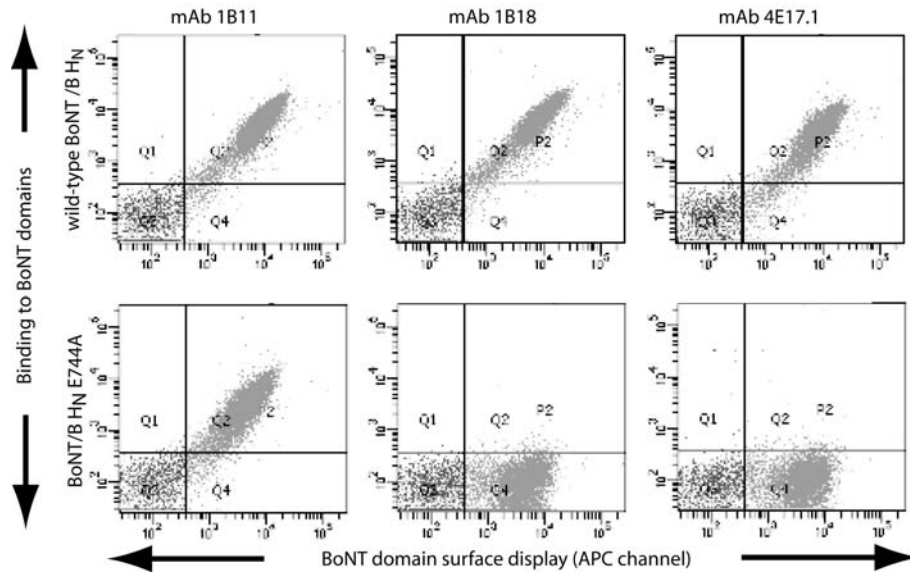
Fig. 5 Fine epitope of 1B18 and 4E17.1 mAbs. Binding of 1B18 and 4E17.1 mAbs to wild-type BoNT/B H_N and the BoNT/B H_N E747A mutant. As a control binding of the H_N mAb 1B11 is also shown. 1B11 binds to both the wild-type and mutant H_N, whereas neither 1B18 nor 4E17.1 bind to the H_N E747A mutant. The results indicate that the fine epitope of both 1B18 and 4E17.1 is located around H_N amino acid E747.
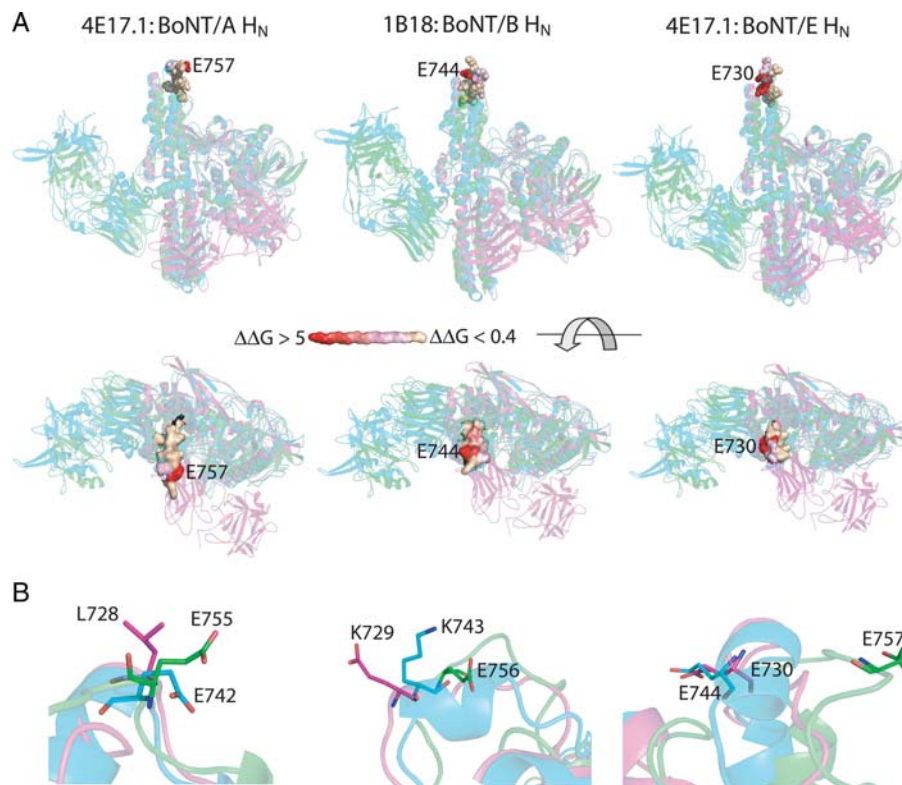
Fig. 6 Model of the functional binding epitopes of 1B18 and 4E17.1 mAbs. (A) The epitopes of 1B18 on BoNT/B (center panels) and 4E17.1 on BoNT/A (left panels) and BoNT/E (right panels) are indicated. The X-ray crystal structures of BoNT/A (green), BoNT/B (cyan) and BoNT/E (magenta) were structurally aligned on amino acid 757 of BoNT/A and are shown as ribbon diagrams. The middle set of panels represent the upper panels rotated 90° to give a birds-eye view of the mAb epitope. The 1B18 and 4E17 epitopes are shown in surface projection colored from red to wheat to indicate the $\Delta\Delta G$ values from Table IV. The lower set of panels show the side chains of amino acids E755, E756 and E757 of BoNT/A and their corresponding amino acids in BoNT/B and E on the aligned crystal structures.

those in the tip of the H_N) have relatively high b-factors. Thus, it is possible that the loop at the tip of the H_N is mobile and adapts to the mAbs with a more homologous structure. Alternatively, it is possible that the mAbs adopt different conformations or isomers, as has been shown for an antibody binding both a hapten and a peptide (James *et al.*, 2003). It is also possible that both the mAb and the loop of the toxin domain undergo structural changes simultaneously;
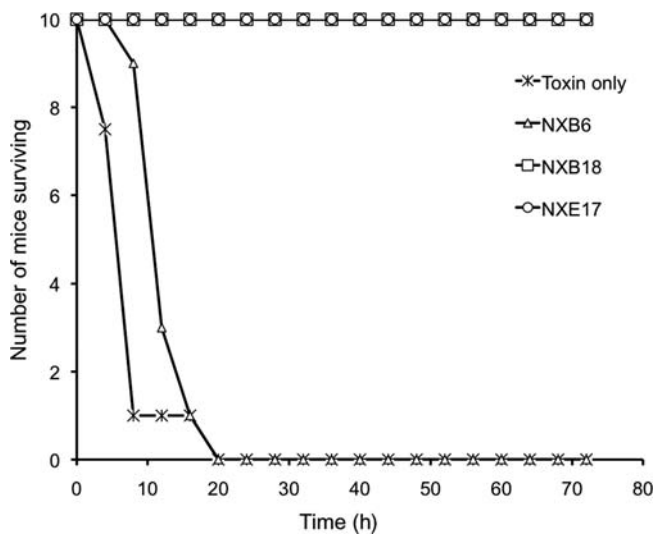
Fig. 7 Antibody protection of mice against challenge with BoNT/B or E. Twenty-five micrograms of the indicated mAb was mixed with 200 mouse LD$_{50}$ of either BoNT/B (4B6.1 and 2B18.1) or BoNT/E (4E17.1) and injected intraperitoneally into each of 10 mice. The number of mice surviving versus time is plotted. The toxin only control is for BoNT/B.

in the line of an induced-fit model, to facilitate the selective binding. A full understanding of the cross-serotype reactivity will await solution of their co-crystal structure with BoNT, studies that are underway.

The identification of cross-serotype binding mAbs has implications for the diagnosis and treatment of botulism, as well as for the therapeutic use of BoNTs. With respect to diagnosis, many diagnostic platforms use mAbs to capture or detect BoNT (Varnum et al., 2006; Kalb et al., 2008, 2009; Grate et al., 2009; Warner et al., 2009). For example, Kalb et al. (2008) at the Centers for Disease Control and Prevention have developed a mass spectrometry-based assay that uses mAbs to capture BoNT from complex mixtures such as serum or stool. mAb captured BoNT is then incubated with substrate and substrate cleavage detected by mass spectrometry, achieving sensitivities greater than the mouse assay, the current gold standard. Use of BoNT cross-reactive mAbs greatly simplified the assay by requiring only a single mAb for multiple serotypes (Kalb et al., in press). With respect to treatment, high-affinity cross-reactive mAbs, such as 4E17.1 could be used to neutralize both BoNT/A and E, reducing the number of mAbs required to achieve broad serotype coverage (Nowakowski et al., 2002). In summary, although cross-serotype reactive BoNT mAbs are rare, they should prove especially useful for the diagnosis and treatment of botulism.

Materials and methods

Oligonucleotides

V_L-shuffled library construction.

4E17 VH amplification from pYD2
  PYDFOR1: 5′-GTCGATTTTGTTACATCTACAC-3′
  LinkRev: 5′-CGACCCGCCACCGCCAGAGCCACCTCC GCC-3′
VL repertoire amplification from immune human scFv libaries in pYD2

LinkFor: 5′-GGCGGAGGTGGCTCTGGCGGTGGCGGGT CG -3′
  PYDRev: 5′-GTCGATTTTGTTACATCTACAC-3′
1B18 VH amplification from PYD2
  HuVH1aBACKFabGap: 5′-AAGGCTCTTTGGACAAGA GAAACTCTGGATCCCAGGTGCAGCTGGTGCAGT CTGG-3′
  HuJH1-2ForFabGap: 5′- GTGCCAGGGGGAAGACCGA TGGGCCCTTGGTGCTAGCTGAGGAGACGGTGAC CAGGGTGCC-3′

4E17.1 CDRH1, 2 and 3 library construction. Primers designed to introduce diversity into corresponding CDR

4E17mutH1Rev: 5′GACCCAAGTCATCCA**52354254451253 3**TCCGGTGGCTGCACA-3′
4E17mutH2Rev: 5′AGAGTCCACGTAAAA**522524532**GCC GTC**513522**TATGTTGGCCACCCA-3′
4E17mutH3Rev: 5′GGGACTCAGCCACCC**522521544544** CCA**523**AAGTCTCGCACAGTA-3′

where 1, 70%A + 10%T + 10%G + 10%C; 2, 70%T + 10%A + 10%G + 10%C; 3, 70%G + 10%A + 10%T + 10%C; 4, 70%C + 10%A + 10%T + 10%G; 5, 50%G + 50%C

Primers designed to amplify the second fragment from 4E17.1 scFv

4E17H1For: 5′TGGATGACTTGGGTCCGGCAGGCTCCAG GG-3′
4E17H2For: 5′TTTTACGTGGACTCTGTGAAGGGCCGAT TC-3′
4E17H3For: 5′GGGTGGCTGAGTCCCTGGGGCCAGGGA ACC-3′

Cloning of BoNT/E domains.

BoNTELCFor: 5′ ATATATAATCCATGGCT<u>ATGCCGAAA ATCAACTCGTTCAAC</u>-3′
BoNTELCBack: 5′-TAGTATATATGCGGCCGC<u>GTCAGC GTTAAAGGCATCCGTAAG</u>-3′
BoNTEHN5For: 5′- ATATATAATCCATGGCT<u>TCCATCT GCATCGAGATCAACAAC</u> -3′
BoNTEHNBack 5′- TAGTATATATGCGGCCGC<u>GGATCCG TGCTGGATGATGTAGTT</u> -3′
BoNTEHCFor: 5′ ATATATAATCCATGGCT<u>GGAGAGAGT CAGCAAGAACTAAAT</u>-3′
BoNTEHCBack 5′-TAGTATATATGCGGCCGC<u>TTTTTCTT GCCATCCATGTTCTTC</u>-3′

Underlined sequence anneals to the relevant sequence of the BoNT domain gene.

Cell lines, media, toxins and antibodies

Yeast strain EBY100 (GAL1-AGA1TURA3 ura3-52 trp1 leu2D1 his3D200 pep4THIS2 prb1D1.6R can1 GAL) was maintained in YPD medium (*Current Protocols in Molecular Biology*, John Wiley and Sons, Chapter 13.1.2). EBY100 transfected with expression vector pYD2 (Razai et al., 2005) was selected on selective dextrose casamino acid (SD-CAA) medium (*Current Protocols*, Chapter 13.1.2). ScFv yeast surface display was induced by transferring yeast cultures

from SD-CAA to selective galactose (SG)-CAA medium (identical to SD-CAA medium except the glucose was replaced by galactose) and grown at 20°C for 24–48 h as described previously (Feldhaus *et al.*, 2003). Bacterial strain *E. coli* DH5α was used for cloning and preparation of plasmid DNA. Pure BoNT types A1, A2, B1, E3 and proteolytic F Langeland were purchased from Metabiologics. Pure BoNT/E1 complex was purchased from WAKO Chemicals. Pure BoNT/A3, B2, bivalent B3 and non-proteolytic B4 were purified from their respective strains. Crude BoNT/E2 was prepared from *C. botulinum* CDC 5247 and was used unpurified. SV5 antibody was purified from hybridoma supernatant using Protein G and directly labeled with Alexa-488 or Alexa-647 using a kit provided by the manufacturer (Molecular Probes).

Initial characterization of a panel of BoNT antibodies

A panel of 35 scFvs binding BoNT/A, B or E were studied. Thirty-three mAbs were generated from humans immunized with pentavalent botulinum toxoid, and two mAbs were generated from a mouse immunized with BoNT/A holotoxin (S25 and C25). All mAbs were isolated from scFv gene libraries generated from immune B-cells and displayed on either the surface of phage or the surface of yeast (Amersdorfer *et al.*, 1997, 2002; Levy *et al.*, 2007, and unpublished data). Serotype specific mAbs were isolated by selecting libraries on, either BoNT/A, B or E. For phage-displayed scFv (C25 and S25), the scFv gene was subcloned into yeast display vector pYD2 (Razai *et al.*, 2005). Each yeast-displayed scFv in EBY100 was grown and induced as described previously (Razai *et al.*, 2005). For cross-reactivity testing, 2.5×10^5 yeast cells were incubated with 50 µl of 100 nM BoNT/A1, B1 or E1, for 1 h at room temperature with mild rocking. Cells were pelleted and washed with 0.5 ml of cold fluorescent-activated cell sorting (FACS) buffer (1 mM MgCl$_2$, 0.5 mM CaCl$_2$, 0.5% BSA) and resuspended in 100 µl of the corresponding secondary antibodies. For secondary antibodies, two IgGs binding non-overlapping BoNT epitopes and labeled with Alexa-647 were used (for BoNT/A1, ING2 and RAZ1, for BoNT/B1, 4B6 and 1B10.1 and for BoNT/E3 3E2 and 3E6.1). The yeast display level was quantitated by co-staining with SV5-Alexa-488. After 40 min incubation at 4°C, cells were washed once with FACS buffer and analyzed by flow cytometry in a BD FACS Aria.

Measurement of yeast-displayed scFv affinity for BoNTs

Quantitative equilibrium binding was determined using yeast-displayed scFv and flow cytometry as described previously (Razai *et al.*, 2005). In general, six to eight different concentrations of pure BoNT were utilized spanning a range of concentrations from 10 times above to 10 times below the K_D. Incubation volumes and number of yeast stained were chosen to keep the number of antigen molecules in 10-fold excess above the number of scFv, assuming 5.0×10^5 scFv/yeast. Incubation times were chosen based on anticipated times to equilibrium calculated using approximations of the anticipated association rate constant (k_{on}) and dissociation rate constant (k_{off}; Razai *et al.*, 2005). Binding of BoNT to yeast-displayed scFv was detected using a 1:500 dilution of 1 mg/ml of mAb binding a non-overlapping BoNT epitope (RAZ1 for BoNT/A1, 4B6.1 for BoNT/B and 3E2 for BoNT/E)

labeled with Alexa-647. To quantify the protein-ligand affinity constant (K_D) within the surface display context, only the scFv displaying yeast (SV5 binding) were included in the analysis by co-staining with SV5-Alexa-488. Each K_D was determined in triplicate, three separate inductions and measurements.

Construction and sorting of chain shuffled yeast antibody libraries

A 1B18 V_L chain shuffled Fab library was created by using yeast mating as described in Lou *et al.* (2010). Briefly, the 1B18 V_H gene was amplified from the scFv in pYD2 using HuVH1aBACKFabGap and HuJH1-2ForFabGap primers and cloned by gap repair (Weaver-Feldhaus *et al.*, 2004) into pPNL20 in yeast strain JAR300. To create the chain shuffled library, a human V_L library in strain YVH10 was mated with the 1B18 V_H in JAR300 as previously described (Lou *et al.*, 2010) to create a library of size 2×10^7 transformants. A 4E17 V_L chain shuffled scFv library was created by polymerase chain reaction (PCR) amplifying the V_k gene repertoires from four human immune scFv libraries constructed from humans immunized with pentavalent BoNT toxoid in pYD2 by using *Pfu* polymerase (Stratagene) and primers LinkFor and PYDRev. To further increase V_L diversity, the V_L repertoire from a large non-immune scFv phage antibody library transferred from the phagemid vector pHEN1 and cloned into pYD2 was also utilized (Sheets *et al.*, 1998). 4E17 V_H DNA was amplified from the scFv gene in pYD2 using a 5′ primer that annealed upstream of the V_H gene (PYDFor1) and a 3′ primer that annealed in the linker gene between the V_H and V_L genes (LinkRev). Gel-purified 4E17 V_H gene was mixed with the gel-purified V_L repertoires and combined with NcoI and NotI digested pYD2 vector DNA. This mixture was used to transform LiAc-treated EBY100 cells, by three fragment gap repair. Library size was measured as 3.3×10^7 transformants.

To select higher affinity Fab or scFv, V_L shuffled libraries were grown and Fab or scFv display induced as described previously (Razai *et al.*, 2005; Lou *et al.*, 2010). Yeast were stained with BoNT/B1, E3 or F at a concentration 10 times greater than the K_D of the yeast-displayed parental scFv and equal to the K_D for the first two rounds of sorting, respectively, with the majority of BoNT binding yeast collected. Subsequent rounds of sorting were increasingly stringent with the BoNT concentration decreased and less than 1% of the yeast collected. A total of four to six rounds of sorting were performed, after which the sort output was plated and individual yeast-displayed scFv analyzed. Ten individual clones were characterized by DNA sequencing of the scFv or Fab gene and the affinity for BoNT determined as described previously (Razai *et al.*, 2005, #16).

Construction and sorting of mutagenic CDRH1 4E17.1 scFv yeast display library

A library of 4E17.1 scFv CDRH1 site-directed mutants was constructed using parsimonious mutagenesis as described previously (Schier *et al.*, 1996a,b). Briefly, a partially degenerate oligonucleotide primer (4E17mutH1rev) was designed to introduce mutations into five amino acids (PSGSH) located in CDR H1. The primer was designed to have a bias for 25–50% wild-type amino acid at each position depending on codon usage (Garcia-Rodriguez *et al.*, 2007). The

degenerate primer and the corresponding primer PYDFOR were used to PCR amplify a portion of the V_H gene and 5′ upstream sequence in pYD2 using the 4E17.1 scFv in pYD2 as template. A second PCR amplification was performed on the same template using a forward primer complementary to the 15 nucleotides at the 5′ end of corresponding 4E17mutHrev and the primer PYDRev. The two PCR products comprising the whole 4E17.1 scFv gene with the diversified V_H CDR1 were gel purified and further spliced together using PCR. The spliced scFv gene repertoire was combined with Nco1/Not1 digested pYD2 and used to transform EBY100 using gap repair. Library size was 3.4×10^7. To select for more broadly reactive scFv, the following sorts were done: first round, 1 nM BoNT/E3; second round, 20 nM BoNT/B1; third round, 5 nM BoNT/B1 and 200 pM BoNT/E3; and fourth round, 2 nM BoNT/B1 and 0.5 nM BoNT/E3. The last two sorts were performed by labeling BoNT/B1 and E3 with different Alexa fluorophores. After the fourth round of sorting, eight clones were individually analyzed and the DNA sequence showed that 1–2 mutations were found in all clones, with the mutation S30Q being present in all clones.

Construction and sorting of mutagenic CDRH2 and CDRH3 4E17.4 scFv yeast display libraries

Libraries of 4E17.4 scFv CDRH2 or CDRH3 site-directed mutants were constructed using parsimonious mutagenesis exactly as described above for the 4E17.1 CDRH1 library, except using primers 4E17mutH2rev and 4E17mutH3rev. These primers partially randomized five amino acids in VHCDR2 (NL–TEK) or VHCDR3 (Q-GGYN). After transformation, library sizes were 4.3×10^7 and 5.0×10^7. Each library was selected on BoNT/B and E as described above for the 4E17.1 VHCDR1 library.

Construction of yeast-displayed BoNT/A1, B1 and E1 H_N domains

Yeast-displayed BoNT/A1 and B1 H_C, H_N and L_C have been described previously (Levy et al., 2007; I.N. Geren, submitted for publication). To generate yeast-displayed BoNT/E H_C, H_N and L_C, a synthetic BoNT/E gene (Dux et al., 2006) was PCR amplified using the primer pairs HCFor and HCBack, HNFor and HNBack or LCFor and LCBack and adding the restriction sites NcoI and NotI to the 5' and 3' ends, respectively. PCR BoNT/E domain genes and pYD2 vector were digested with NcoI and NotI and after ligation used to transform E. coli DH5α. Clones containing the correct insert were confirmed by DNA sequencing. Yeast surface display was induced as described previously (Levy et al., 2007). Yeast-displayed alanine mutants of BoNT/A1, B1 and E3 were constructed as described previously (Levy et al., 2007). After induction, alanine mutants of H_N had surface display levels resulting in at least a 1.5-log shift from control when stained with SV5-Alexa-488, comparable with the levels of wild-type BoNT H_N display.

Generation and purification of F_{ab} from IgG

IgG were constructed from scFv or Fab V-genes and stably expressed as human IgG from CHO cells as described previously. Alternatively human IgG1 were transiently expressed from HEK293 cells. IgG were purified using Protein A or Protein G chromatography. F_{ab} fragments were prepared from IgG using immobilized papain (Pierce Biotechnology, IL,

USA). Briefly, IgG was concentrated to ~12 mg/ml in 20 mM phosphate, 10 mM EDTA, pH 7.0, then added to an equal volume of immobilized papain resin (washed with 20 mM phosphate, 10 mM EDTA, 20 mM cysteine pH 7.0) and incubated at 37°C for 16 h. The immobilized papain was removed by centrifugation, and the digest supernatant was dialyzed against 10 mM MES, pH 5.6. The F_{ab} fragment was separated from undigested IgG and F_C fragments by cation exchange chromatography (HiTrap SP HP, GE Healthcare, NJ, USA) using a salt gradient. The purified F_{AB} was then dialyzed against PBS and stored at −80°C. To ensure that the F_{AB} retained the expected affinity, the K_D of 1B18 and 4E17.1 IgG and F_{ab} fragments for yeast-displayed H_N A1 were measured by flow cytometry. The measured K_D values for 1B18 and 4E17.1 F_{ab} (598 and 1.83 pM, respectively) were comparable to the IgG solution K_D measured previously (864 and 45 pM, respectively).

Measurement of the affinity of F_{ab} for yeast-displayed BoNT H_N mutants

The dissociation equilibrium constants (K_D) of 1B18 or 4E17.1 F_{ab} for wild-type and alanine mutants of yeast-displayed BoNT H_N were measured by flow cytometry on a FACS Aria flow cytometer (BD Biosciences). First, EBY100 yeast cultures harboring the pYD2/HN wild-type or the pYD2/HN alanine mutant plasmids were grown and induced as described previously (Levy et al., 2007). Aliquots of 1.0×10^5 induced yeast cells (~.005 OD_{600} mL^{-1}) were washed in FACS buffer and incubated with dilutions (ranging from 1 μM to 1.6 pM) of 1B18 or 4E17.1 F_{ab} such that the K_D would be spanned by 10-fold, where possible. Incubation volumes were chosen to ensure that a 5-fold molar excess of the antibody (ligand) over the displayed moiety (H_N) would be maintained. For this purpose, it was assumed that ~10^5 H_N copies were displayed on the yeast surface. Incubation with 1B18 or 4E17.1 F_{ab} was allowed to proceed for 4 h. Cells were then washed in FACS buffer and resuspended in allophycocyanin-conjugated Fab-specific goat-anti-human F(ab)'2 at 1:500 dilution in FACS buffer. To accurately determine the K_D of 1B18 and 4E17.1 Fab within the surface display context, we included only H_N displaying yeast in the analysis by co-staining with SV5 (Alexa-647) mAb.

Calculation of the change in free energy of binding of BoNT H_N alanine mutants

For each BoNT/A1, B1 and E1 H_N alanine mutation, the change of free energy ($\Delta\Delta G_{mut-wt}$) between the BoNT H_N alanine (Ala) mutant relative to that of the wild type (wt) was calculated using the following standard formula and using the previously measured K_D constants: $\Delta\Delta G_{mut-wt} = RT \ln(K_{D,Ala}/K_{D,wt})$.

Measurement of in vivo toxin neutralization

In vivo toxin neutralization was measured as described previously (Smith et al., 2005). Briefly, 0.5–50 μg of the appropriate IgG or antitoxin were added to the indicated number of mouse LD_{50} of BoNT/A1 or B1 neurotoxin complex in a total volume of 0.5 ml of gelatin phosphate buffer and incubated at RT for 30 min. For combinations of two or three mAbs, mAbs were combined in an equimolar ratio before adding to toxin. The mixture was then injected

intraperitoneally into female CD-1 mice (16–22 g on receipt). Mice were studied in groups of 10 and were observed at least twice daily. The final death tally was determined 5 days after injection except where indicated otherwise. Studies using mice were conducted in compliance with the Animal Welfare Act and other Federal statutes and regulations relating to animals and experiments involving animals and adhere to principles stated in the *Guide for the Care and Use of Laboratory Animals*, National Research Council (1996). The facility where this research was conducted is fully accredited by the Association for Assessment and Accreditation of Laboratory Animal Care International.

Supplementary data

Supplementary data are available at *PEDS* online.

Acknowledgements

Funding

References

Amersdorfer,P., Wong,C., Chen,S., Smith,T., Desphande,S., Sheridan,R., Finnern,R. and Marks,J.D. (1997) *Infect. Immun.*, **65**, 3743–3752.

Amersdorfer,P., Wong,C., Smith,T., Chen,S., Deshpande,S., Sheridan,R. and Marks,J.D. (2002) *Vaccine*, **20**, 1640–1648.

Arnon,S.A., Schecter,R., Inglesby,T.V., *et al.* (2001) *JAMA*, **285**, 1059–1070.

Bagramyan,K., Barash,J.R., Arnon,S.S. and Kalkum,M. (2008) *PLoS ONE*, **3**, e2041.

Bozheyeva,G., Kunakbayev,Y. and Yeleukenov,D. (1999) *Center for Nonproliferation Studies*. Monterey Institute of International Studies, Monterey, CA.

Centers for Disease Control and Prevention. (1998) U.S. Department of Health and Human Services, Public Health Service, Atlanta, GA, http://www.bt.cdc.gov/agent/botulism/index,asp.

Clackson,T., Hoogenboom,H.R., Griffiths,A.D. and Winter,G. (1991) *Nature*, **352**, 624–628.

Dolly,J.O., Black,J., Williams,R.S. and Melling,J. (1984) *Nature*, **307**, 457–460.

Dong,M., Yeh,F., Tepp,W.H., Dean,C., Johnson,E.A., Janz,R. and Chapman,E.R. (2006) *Science*, **312**, 592–596.

Dux,M.P., Barent,R., Sinha,J., *et al.* (2006) *Protein Expr. Purif.*, **45**, 359–367.

Eswaramoorthy,S., Kumaran,D. and Swaminathan,S. (2001) *Acta Crystallogr. D Biol. Crystallogr.*, **57**, 1743–1746.

Feldhaus,M.J., Siegel,R.W., Opresko,L.K., *et al.* (2003) *Nat. Biotechnol.*, **21**, 163–170.

Figini,M., Marks,J.D., Winter,G. and Griffiths,A.D. (1994) *J. Mol. Biol.*, **239**, 68–78.

Fischer,A., Garcia-Rodriguez,C., Geren,I., Lou,J., Marks,J.D., Nakagawa,T. and Montal,M. (2008) *J. Biol. Chem.*, **283**, 3997–4003.

Garcia-Rodriguez,C., Levy,R., Arndt,J.W., Forsyth,C.M., Razai,A., Lou,J., Geren,I., Stevens,R.C. and Marks,J.D. (2007) *Nat. Biotechnol.*, **25**, 107–116.

Gill,M.D. (1982) *Microbiol. Rev.*, **46**, 86–94.

Grate,J.W., Warner,M.G., Ozanich,R.M. Jr., *et al.* (2009) *Analyst*, **134**, 987–996.

Hill,K.K., Smith,T.J., Helma,C.H., *et al.* (2007) *J. Bacteriol.*, **189**, 818–832.

James,L.C., Roversi,P. and Tawfik,D.S. (2003) *Science*, **299**, 1362–1367.

Kalb,S.R., Smith,T.J., Marks,J.D., Hill,K., Pirkle,J.L., Smith,L.A. and Barr,J.R. (2008) *Int. J. Mass Spec.*, **278**, 101–108.

Kalb,S.R., Lou,J., Garcia-Rodriguez,C., *et al.* (2009) *PLoS ONE*, **4**, e5355.

Kalb,S.R., Garcia-Rodriguez,C., Lou,J., Baudys,J., Smith,T.J., Marks,J.D., Smith,L.A., Pirkle,J.L. and Barr,J.R. (2010) *PLoS ONE*, **5**, e12237.

Kumaran,D., Eswaramoorthy,S., Furey,W., Navaza,J., Sax,M. and Swaminathan,S. (2009) *J. Mol. Biol.*, **386**, 233–245.

Lacy,D.B. and Stevens,R.C. (1999) *J. Mol. Biol.*, **291**, 1091–1104.

Lacy,D.B., Tepp,W., Cohen,A.C., DasGupta,B.R. and Stevens,R.C. (1998) *Nat. Struct. Biol.*, **5**, 898–902.

Levy,R., Forsyth,C.M., LaPorte,S.L., Geren,I.N., Smith,L.A. and Marks,J.D. (2007) *J. Mol. Biol.*, **365**, 196–210.

Lou,J., Geren,I., Garcia-Rodriguez,C., *et al.* (2010) *Protein Eng. Des. Sel.*, **23**, 311–319.

Mahrhold,S., Rummel,A., Bigalke,H., Davletov,B. and Binz,T. (2006) *FEBS Lett.*, **580**, 2011–2014.

Middlebrook,J.L. and Franz,J.R. (1997) In Sidell,F.R., Takafuji,E.T. and Franz,D.R. (eds). *Medical Aspects of Chemical and Biologic Warfare.* Office of the Surgeon General, 643–654.

Montecucco,C. and Schiavo,G. (1995) *Quart. Rev. Biophys.*, **28**, 423–472.

NIAID Experts Panel (2004) http://www.niaid.nih.gov/topics/BiodefenseRelated/Biodefense/Documents/bot_toxins.pdf.

Nowakowski,A., Wang,C., Powers,D.B., *et al.* (2002) *Proc. Natl. Acad. Sci. USA*, **99**, 11346–11350.

Razai,A., Garcia-Rodriguez,C., Lou,J., *et al.* (2005) *J. Mol. Biol.*, **351**, 158–169.

Schiavo,G., Benfenati,F., Rossetto,O., Polverino,d.L.P., DasGupta,B.R. and Montecucco,C. (1992) *Nature*, **359**, 832–835.

Schiavo,G., Rossetto,O., Catsicas,S., Polverino,d.L.P., DasGupta,B.R., Benfenati,F. and Montecucco,C. (1993) *J. Biol. Chem.*, **268**, 23784–23787.

Schier,R., Balint,,R.F., McCall,A., Apell,G., Larrick,J.W. and Marks,J.D. (1996a) *Gene*, **169**, 147–155.

Schier,R., McCall,A., Adams,G.P., *et al.* (1996b) *J. Mol. Biol.*, **263**, 551–567.

Sheets,M.D., Amersdorfer,P., Finnern,R., *et al.* (1998) *Proc. Natl Acad. Sci. USA*, **95**, 6157–6162.

Simpson,L.L. (1980) *J. Pharmacol. Expt. Ther.*, **212**, 16–21.

Smith,T.J., Lou,J., Geren,I.N., *et al.* (2005) *Infect. Immun.*, **73**, 5450–5457.

Smith,T.J., Hill,K.K., Foley,B.T., *et al.* (2007) *PLoS ONE*, **2**, e1271.

United Nations Security Council. (1995). Tenth Report of the Executive Committee of the Special Commission Established by the Secretary-General Pursuant to Paragraph 9(b)(I) of Security Council Resolution 687 (1991), and Paragraph 3 of Resolution 699 (1991) on the Activities of the Special Commission. United Nations Security Council, New York, NY.

Varnum,S.M., Warner,M.G., Dockendorff,B., *et al.* (2006) *Anal. Chim. Acta*, **570**, 137–143.

Warner,M.G., Grate,J.W., Tyler,A., Ozanich,R.M., Miller,K.D., Lou,J., Marks,J.D. and Bruckner-Lea,C.J. (2009) *Biosens. Bioelectron.*, **25**, 179–184.

Weaver-Feldhaus,J.M., Lou,J., Coleman,J.R., Siegel,R.W., Marks,J.D. and Feldhaus,M.J. (2004) *FEBS Lett.*, **564**, 24–34.